# MscS is a critical component for osmotic survival of *Vibrio cholerae*

Kristen Ramsey[1,2], Madolyn Britt[1], Joseph Maramba[1], Blake Ushijima[3,4], Elissa Moller[1], Andriy Anishkin[1], Claudia Hase[5], and Sergei Sukharev[1]

[1]Biology, University of Maryland, College Park, MD, [2]Yale University, New Haven, CT, [3]Smithsonian Marine Station, Ft. Pierce, FL, [4]Carlson College of Veterinary Medicine, Oregon State University, Corvallis, OR, [5]Biomedical Sciences College of Veterinary Medicine, Oregon State University, Corvallis, OR

Abstract

Intestinal bacteria, including the facultative pathogen *Vibrio cholerae*, can adapt to a wide range of osmotic environments. In high-osmolarity media, bacteria accumulate small compatible metabolites to maintain turgor pressure, but under drastic osmotic down-shifts bacteria are able to avoid mechanical rupture by rapidly releasing these metabolites through mechanosensitive (MS) channels. Previous experiments on *V. cholerae* have identified two major types of MS channels - MscS and MscL. We functionally examine these channels' specific roles in *Vibrio's* osmotic rescuing via genetic modification, bacterial patch-clamp electrophysiology, and stopped-flow light scattering. The light scattering kinetics revealed that WT *Vibrio* cells were capable of releasing up to 10% of their total non-aqueous content within ~30 ms. To investigate each channel's individual contribution to *V. cholerae's* osmotic permeability response, we generated and characterized the first individual Δ*mscS*, Δ*mscL*, and double Δ*mscL* Δ*mscS* mutants in *V. cholerae* O395. Both mutants lacking MscS exhibited delayed osmolyte release kinetics and decreased osmotic survival rates compared to WT. Surprisingly, the Δ*mscL* mutant had comparable kinetics to WT, but a much higher osmotic survival, whereas Δ*mscS* had low survival, comparable to the double Δ*mscL* Δ*mscS* mutant. The data indicate that MscS is much more efficient in osmotic adjustment and is up-regulated in the absence of MscL, whereas in the absence of the low-threshold MscS, MscL even becomes toxic. Kinetic modeling of the cell swelling process and channel activation reveals the advantage of low-threshold MscS in curbing tension surges in *Vibrio* and its role in proper termination of the osmotic permeability response.

## Introduction

All free-living microorganisms, both commensal and pathogenic, confront environmental challenges involving osmotic up- and down-shifts. This is especially relevant to intestinal microorganisms, which are transferred from host to host primarily through freshwater. Mechanosensitive (MS) channels from MscS and MscL (small-conductance and large-conductance MS channels, respectively) families, acting as osmolyte release valves, have been shown to be critical for osmotic survival (Booth and Blount, 2012; Cox et al., 2018; Levina et al., 1999) . The electrophysiological comparison of wild-types (WT) *Escherichia coli* and *Vibrio cholerae* indicated that both microorganisms easily survive drastic (600-800 mOsm) hypoosmotic shifts, apparently because they have similar compliments of MS channels in their inner membranes (Rowe et al., 2013). However, an explanation for the apparent redundancy of the two channels and precisely how the osmotic rescuing and release occur remains unclear.

Osmotic forces are strong, an accumulation of 0.1 M metabolites inside the cell creates a total of 2.4 atm of pressure. Thus, all free-living microorganisms must have defenses against drastic osmotic changes to survive (Kung et al., 2010). As bacterial membranes are almost freely permeable to water, their sole mechanism for evading osmotic rupture is by reducing the osmotic gradient. This is achieved by expulsion of small osmolytes through two major types of MS channels, MscS and MscL, which open in direct response to membrane tension. Under hyperosmotic conditions, bacteria will accumulate osmolytes compatible with their cellular functions (Wood, 2006; Yancey et al., 1982), such as K+, glycine betaine, and ectoine (Pflughoeft et al., 2003). MscS, the most commonly found member within the MscS family, opens at non-lytic tensions (5-7 mN/m) (Belyy et al., 2010; Sukharev, 2002) and exhibits adaptive behavior that includes inactivation (Akitake et al., 2005). Conversely, MscL, the larger-conductance emergency release valve (Sukharev et al., 1994), opens at near-lytic tensions (10-14 mN/m)(Belyy et al., 2010; Sukharev et al., 1999) and does not inactivate. Since water diffuses directly through the membrane, a sudden dilution of external media leads to rapid swelling and pressure buildup within the cell. To survive and curb the pressure surge, the cell must expel osmolytes at a rate that beats the water influx. Thus, survival under osmotic down-shock is a question of kinetic competition between these two fluxes (Bialecka-Fornal et al., 2015).

MS channels in bacteria were first discovered when the procedure of giant spheroplast preparation was adopted for direct patch-clamp recording (Martinac et al., 1987). Bacterial MS channels from two separate families (Sukharev et al., 1993) were then identified in *E. coli* (Levina et al., 1999; Sukharev et al., 1994) and have since been found all free-living bacteria, both gram negative and gram-positive (Balleza and Gomez-Lagunas, 2009). More attention was given to opportunistic pathogens such as *Pseudomonas aeruginosa* (Cetiner et al., 2017) and *V. cholerae* (Rowe et al., 2013[j]), where these channels were electrophysiologically characterized to some detail. In addition to electrophysiology, the physiological roles of individual bacterial MS channels are typically researched through generation of knock-out (KO) mutants lacking one or more channel[i]. Their osmotic phenotypes are characterized in hypotonic shock survival experiments (Levina et al., 1999), and more recently the application of the stopped-flow technique has been developed to study fast kinetics of osmolyte release (Cetiner et al., 2017; Moller et al., 2023).

*E. coli* is primarily found in normal flora of the gastrointestinal tract, but *V. cholerae*, like many species of *Vibrio*, lives in brackish waters, frequently attached to crustacean shells (Nahar et al., 2011). Being adaptable to both high-salinity and fresh water, toxicogenic strains of *V. cholerae* often cause seasonal outbreaks of cholera in areas where potable, clean water is

unavailable (Emch et al., 2008). *V. cholerae* osmoadaptivity correlates with the presence MscL, which is absent from many strictly marine members in the *Vibrio* genus (Booth and Blount, 2012). It appears to be a key difference that allows *V. cholerae* to colonize and infect the human gut without rupturing (Keymer et al., 2007) during fresh-water transfer between individuals. Although *V. cholerae* pathogenesis is known to be dependent on the presence of various phage-associated virulence factors (Faruque et al., 1998), its easy transfer and propagation appear to be contingent upon the presence of both MscS and MscL.

To achieve a mechanistic understanding of osmoregulation and environmental stability, in this work we generated the first Δ*mscL* and Δ*mscL* Δ*mscS* mutants in *V. cholerae* O395 toxT:lacZ (treated as WT) and characterized them, along with a Δ*mscS* (Hase, 2001) mutant developed in the Dr. Häse laboratory. Each MS channel KO clone, along with WT *V. cholerae*, was subjected to osmotic testing to characterize the channels' individual and collective effects on osmoadaption. The comparison of WT *V. cholerae* O395 with isogenic Δ*mscS*, and the double Δ*mscL* Δ*mscS* mutants revealed that MscS is critical for osmotic survival and the remaining MscL does not functionally substitute for MscS. To single out MscS's function, we independently generated a Δ*mscL* mutant and observed that the Δ*mscL* cells had a fast permeability onset, and the osmotic survival percentage for the mutant was considerably higher than that of WT. This correlated with overexpression of MscS as a compensation for the absent MscL verified by quantitative RT PCR. This work represents the first kinetic description of osmolyte release in *V. cholerae*; it demonstrates the critical role of MscS in the osmolyte release mechanism, and suggests a yet unknown crosstalk between expression regulation of the *mscS* gene and the presence or absence of MscL.

## Materials and Methods

*Strains and Mutant Generation.* The parental *V. cholerae* strain O395 toxT:lacZ (treated as WT), and the Δ*mscS* mutant previously generated from it were received from Dr. Claudia Häse. Using methods adapted from Ushijima et. al (Ushijima et al., 2016), we additionally generated a Δ*mscL* mutant and a double KO Δ*mscL* Δ*mscS* mutant through homologous recombination of a deletion cassette into the relevant *V. cholerae* chromosome. The deletion cassette was delivered via suicide plasmid obtained from conjugation with *E. coli* (EC B3914).

*Osmotic Viability Assays.* To quantify the survival of *V. cholerae* under osmotic stress, each mutant and WT was subjected to rapid down-shock and then measured for survival percentage. Cells were grown in Luria Bertani (LB) media supplemented with NaCl to bring it to 1200 mOsm to early logarithmic phase ($OD_{600}$ ~0.25) and then 30 µL of culture was rapidly pipetted into 5 mL's of either 1200 mOsm LB (non-shock control) or lower osmolarity media to simulate environmental down-shock. Lower osmolarity media ranged between standards of 800 mOsm LB, 600 mOsm LB, and 400 mOsm LB, then decreased by 50 mOsm until 150 mOsm LB. Inoculated culture was incubated at room temperature for 15 minutes, then 30 µL was quickly diluted into a fresh 5 mL of the same osmolarity as the initial shock. Cells were then plated in duplicates and all resulting colonies manually counted. To determine percent survival, each colony count was normalized to counts in non-shock controls. The average survival rates and standard deviations were based on seven independent experiments.

*The Light-Scattering Stopped-Flow Experiments.* To observe and characterize the osmolyte release kinetics of each MS channel down-shock, we employed rapid-mixing osmolyte efflux stopped-flow technique with light scattering detection. The technique allows us to discern the characteristic times taken by sequential processes of bacterial cell swelling, channel opening, osmolyte and water release and finally either cell recovery or mechanical damage by the down-shock.

For down-shocks, *V. cholerae* cells were grown in 1200 mOsm LB media then briefly spun down and resuspended in the resulting supernatant to an $OD_{600}$ of 2.0 to concentrate them. Once concentrated, cells were rapidly mixed with diluted media in a 1:10 ratio in a two-syringe stopped-flow machine (Bio-Logic SFM-2000) with an 80 µl optical mixing chamber (Figure S1). The stopped-flow machine was equipped with a modular spectrophotometer to measure the small-angle (5-13$^{o}$) light scattering as a result of changes in cell size and refractive index (n) reflecting the concentration of internal non-aqueous components ("dry weight"). Both cell size and n change due to water influx and subsequent osmolyte release when cells are rapidly shocked in lower osmolarity media.

For down-shock experiments, 1200 mOsm LB media was diluted with sterile deionized water to lowered osmolarities of 150, 300 mOsm, 450, 600, and 900 mOsm, which were used for shocks, in addition to deionized distilled water ($ddH_2O$). The 1:10 ratio of cells in 1200 mOsm media to diluted media thus created final down-shock osmolarities of approximately 100, 250, 400, 500, 650, and 900 mOsm.

Light-scattering traces was collected over a period of 4 seconds, with sampling every 10 milliseconds, for a total of 8001 data points per shock. Cells were shocked sequentially into each diluted media with five technical replicates per trial and averaged. Down-shock trials were repeated with at least six biological replicates per clone. Readings of background scattering were done with the pure, cell-less supernatant medium in which cells were grown. These were later subtracted from readings of the *V. cholerae* cellular shocks as a baseline.

Down-shock scattering traces were fit from the initialization of MS channels opening to the point where osmotic pressure lessens and membrane tension reaches below subthreshold level and channels close (typically occurring in 0.5 seconds). Fitting was performed on MATLAB, to the previously derived (Cetiner et al., 2017; Moller et al., 2023), simplified version Rayleigh-Gans equation, $S = I(m_i + m_{p_0} * e^{(t_0 - t)/\tau})^2$, where S is the scattering and $m_i$ and $m_p$ are the fractions of impermeable and permeable osmolytes in masses, respectively. $t_0$ designates the start of the fit, and $\tau$ is the rate of osmolyte release. $t_0$ was chosen starting at the steepest negative slope (representative of MS channels opening) and fits then continued until this slope leveled off, when channels were observed to close. The analysis of light scattering traces included determination of the extent of initial cell swelling (ES), time to release onset (tro), time to the steepest point and the slope at the end of the trace.

In addition to these parameters, we also determined the water permeability coefficient of *V. cholerae* cells in osmotic up-shock stopped-flow experiments as described in the Supplement.

*Spheroplast Preparation and patch-clamp.* To generate giant spheroplasts for patch-clamp characterization, we adapted a previous *V. cholerae* spheroplast preparation technique[2] used by our colleagues to make it more amenable to our selected O395 strain.

*RT-qPCR*. The WT and ΔmscS strains were grown in LB to the mid-log phase ($OD_{600}$ of ~0.25). Total RNA was extracted from cell cultures using the Monarch Total RNA Miniprep Kit (New England Biolabs) according to the manufacturer's protocol. The concentration of RNA was

measured with the NanoDrop OneC (Thermo Fisher Scientific) with an average yield of 185 ng/uL. RNA samples were then reverse transcribed into cDNA using the qScript cDNA Synthesis Kit (Quantabio), resulting in a final concentration of 10 ng/uL. The reverse transcription reaction was carried out at 22°C for 5 min, 42°C for 30 min, and 85°C for 5 min. RT-qPCR was carried out on a Roche LC480 using the PowerUp SYBR Green Master Mix (Thermo Fisher Scientific) according to the manufacturers protocol. Five technical replicates were run for four biological replicates of each strain with primers for both MscS and adk. The experimental cycling conditions were 50°C for 2 min, then 95°C for 2 min, followed by 40 cycles of 95°C for 15 s, 60°C for 15 s, and 72°C for 1 min. Data are presented as expression fold change using the $2^{-\Delta\Delta CT}$ method relative to the consistently expressed housekeeping gene adenylate kinase, adk (Octavia et al 2013; Livak and Schmittgen, 2001). The error shown in Fig xx is the standard deviation between replicates. A one-tail two-sample t test assuming unequal variances was performed to determine significance. Primer efficiency was determined using cDNA from both strains diluted in a 1:10 dilution scheme resulting in concentrations ranging from 1 ng/µL to 0.00001 ng/µL with six technical replicates for each primer. (Wong and Medrano, 2005). The cycling conditions were 95°C for 5 min followed by 40 cycles of 95°C for 5 s and 60°C for 30 s. A melt curve was run after the cycles for both the experimental conditions and the primer efficiency consisting of 95°C for 5 s, 65°C for 1 min, and 97°C with a ramp rate of 0.11°C/s. Both the primer efficiency data and the experimental data were analyzed using Abs Quant/Fit Points to determine the Ct's and Tm Calling to visualize melt curves and confirm that only one amplicon was present. The averages were taken between the technical replicate Ct's. The primer efficiency was 2.076319 (105.35%) with a slope of -3.1515 for the MscS primers and 2.149385 (107.05%) with a slope of -3.0092 for the adk primers. Based on these efficiencies and the average Ct's, the relative expression ratio was calculated using the equation $ratio = \frac{(E_{target})^{\Delta Ct_{target}}}{(E_{reference})^{\Delta Ct_{reference}}}$, where E is the primer efficiency $E = 10^{-1/slope}$. See Supplemental Figure xx for the primers and primer efficiency plots.

Andriy: Kinetic fitting with COPASI (Hoops et al., 2006; Mendes et al., 2009)

Results

*Generation of ΔmscL and double ΔmscS/ΔmscS deletion mutants in V. cholerae 0395 and their primary characterization*

V. cholerae strain O395 toxT::lacZ was taken as WT and used as the parent strain for KO generation. All mutations were done by inserting gene deletion cassettes containing antibiotic resistance into the ORFs of respective genes. The suicide vector pBU236 containing the *mscL* (VCA0612) gene deletion cassette was conjugated into *V. cholerae* WT and the previously generated *V. cholerae* Δ*mscS* via tri-parental conjugation to generate single and double channel knockouts. The plasmid is incorporated into the genome by homologous recombination and a double cross-over event results in successful knockout mutations.

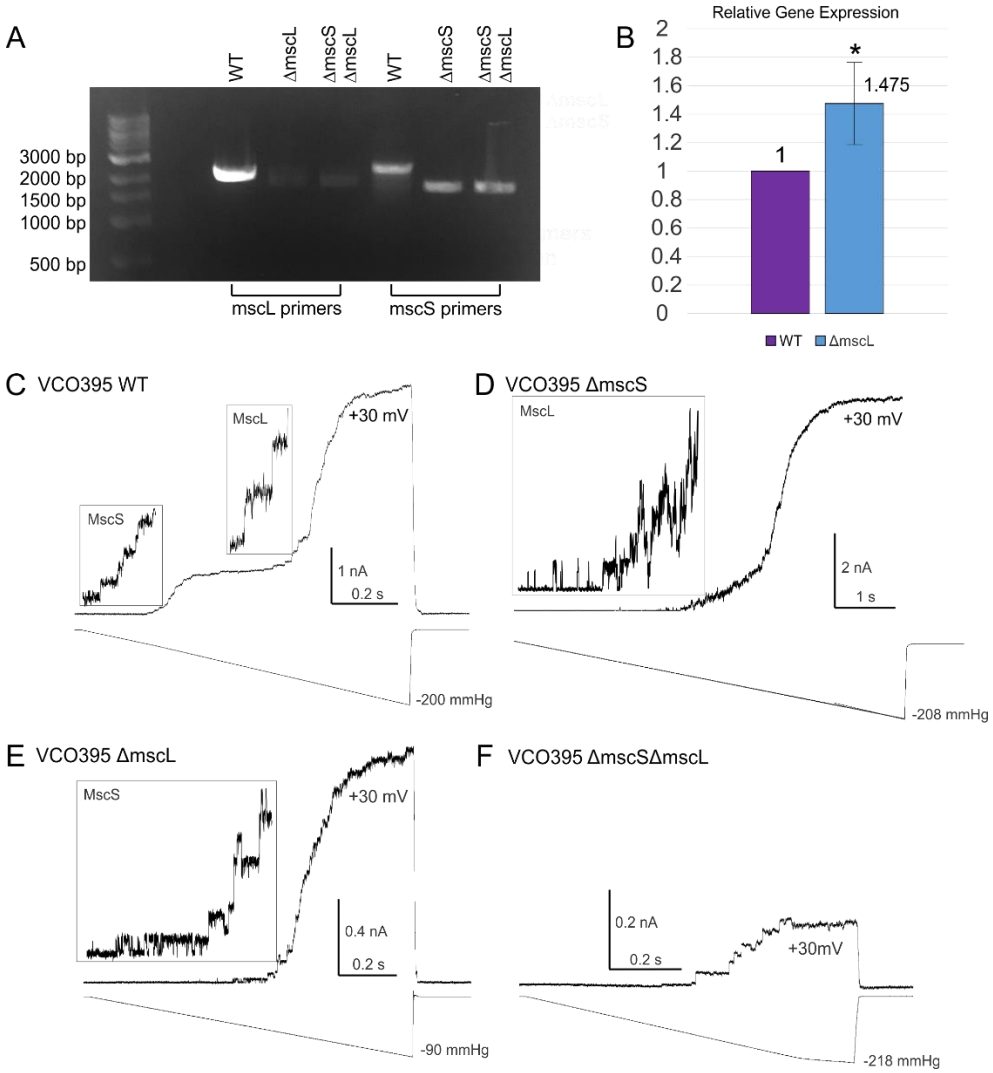


Figure 1. Characterization of Δ*mscL* and Δ*mscL* Δ*mscS* mutants in *V. cholerae* 0395. (A) The gel shows the PCR bands generated with diagnostic primers. (B) qRT-PCR was preformed to verify the overexpression of MscS observed in the electrophysiological characterization of the ΔmscL strain Six independent experiments gave a ratio of 1.475 ± 0.289. Statistically

significant (P = 0.02) expression level when compared to the WT strain is represented with an asterisk. (E). (C-F) Electrophysiological characterization of WT and KO strains by patch-clamp recordings from giant VC spheroplasts. (C) WT strain shows a characteristic 'double wave' generated by the populations of low-threshold (MscS) and high-threshold (MscL) channels. (D-E) The Δ*mscL* and Δ*mscS* strains generate single waves reflecting the remaining type of channels. (F) The double Δ*mscL* Δ*mscS* shows remnant channels without the characteristic waves of MscS and MscL.

Prior to measuring the osmolyte release rates during osmotic shock and resultant survival rates, we confirmed the status of each clone as a true KO mutant by subjecting them to PCR and electrophysiological patch-clamp characterization. For PCR, screening primers were designed to bind upstream and downstream of the gene of interest such that successful KOs would result in PCR product sizes that were smaller than PCR products containing the full gene. Based on the location of the primers, the size of the WT *V. cholerae* O395 genes, and the sizes of the knockout cassettes, the band sizes for mscS present, mscS absent, mscL present, and mscL absent were 2510, 1693, 2265, and 1854 base pairs respectively. The gel in Figure 1A shows the results of WT, Δ*mscS*, Δ*mscL*, and Δ*mscL* Δ*mscS* mutants screened with two sets of primers testing for the presence of the *mscS* and *mscL* genes. For all mutants, the screening primers result in bands that are smaller than their WT counterpart controls, indicating successful gene disruption. Additionally, successful Kos were confirmed in patch clamp by testing for the presence or absence of channel characteristics that are unique to either MscS or MscL (Figure 1 C-F). As expected, WT exhibited two separate, distinct waves of channel activation under an increasing pressure ramp (Figure 1C). The initial channel activation at a lower threshold tension is MscS. As pressure increased and near-lytic tension was reached, a second wave can be seen, representing MscL opening. Conversely, in patch-clamp experiments on our Δ*mscS* clone, we only observed one single wave of activation (Figure 1D). As this activation wave was large and occurred at higher pressure, similar to that of MscL in WT *V. cholerae* O395, we can conclude that the only major channel activity present in Δ*mscS* is indeed MscL, and that there are no obvious channels with MscS-like activity (Figure 1E). Similarly, patch-clamp experiments run on our Δ*mscL* clone also showed a single wave of activation, this one at low pressures. The lower pressure wave is representative of MscS activation. Interestingly, in double knock-out spheroplasts we still observed some small-conductance and low-threshold channel activity (Figure 1E) that may represent the product of one of the remaining *mscS*-like genes such as the putative mechanosensitive channel protein given by accession ABQ22121.1 (292 aa, 37% identity to *E. coli* MscS).

*Characterization of V. cholerae O395 deletion mutants using stopped-flow*

To understand the contributions each MS channel provides to the overall hypoosmotic permeability response, all KO strains were subjected to rapid-dilution stopped-flow experiments to observe the kinetics of osmolyte release and correlate these kinetics with osmotic survival.

We should remember that according to Rayleigh-Gans theory (Koch, 1961; Koch et al., 1996), the forward scattering is proportional to the sixth power of the cell radius and to the square of the ratio of refractive indexes inside and outside the cell. The refractive index inside the cell, in turn, is directly proportional to the weight fraction of non-aqueous compounds (Moller et al., 2023). Figure 2 depicts the typical scattering kinetics that result from fast (8 ms) mixing of a suspension of WT *V. cholerae* O395 pre-grown in 1200 mOsm LB into a 400 mOsm medium. The trace exhibits an ~ 70 ms-long nearly linear decline in scattering representing initial swelling of

the cell resulting in modest cytoplasm dilution leading to a drop of refractive index **n**. Swelling generates tension in the inner membrane which activates MS channels. The region of the curve with the steepest slope is fitted with the simplified Rayleigh-Gans equation ($S = I(m_i + m_{p_0} * e^{(t_0 - t)/\tau})^2$) in order to extract the time constant of release. The scattering level at the end of the trace reflects the fraction of remaining (channel-impermeable) intracellular osmolytes contributing to the refractive index. This end level relative to the initial level also represents the fraction of permeable osmolytes that have exited the cell.

Vertical and horizontal lines in Figure 2 separate the scattering trace into distinct segments, beginning with the downward swelling phase, after which the trace shows a 'break', marked as time to release onset (tro**)**, which is the minimum of the second derivative. The trace then enters the release phase by increasing its downward slope and passing through the steepest point. The minimum of the first derivative delineates the time to the steepest point (tsp). The curve then gradually flattens signifying the end of release and membrane resealing. The parameters of the release phase such as extent of swelling (ES), fraction of permeable osmolytes (FP), and slope at the end are quantifiable with the aid of calibration curves calculated according the Rayleigh-Gans theory (ref, supplement). They tell us to what degree the cell increases its volume before tension in the inner membrane reaches the threshold and the channels open, how quickly they release excessive osmolytes, and what fraction of internal non-aqueous content leaves the cell. The slope at the end of the trace indicates the residual permeability and the quality of resealing.

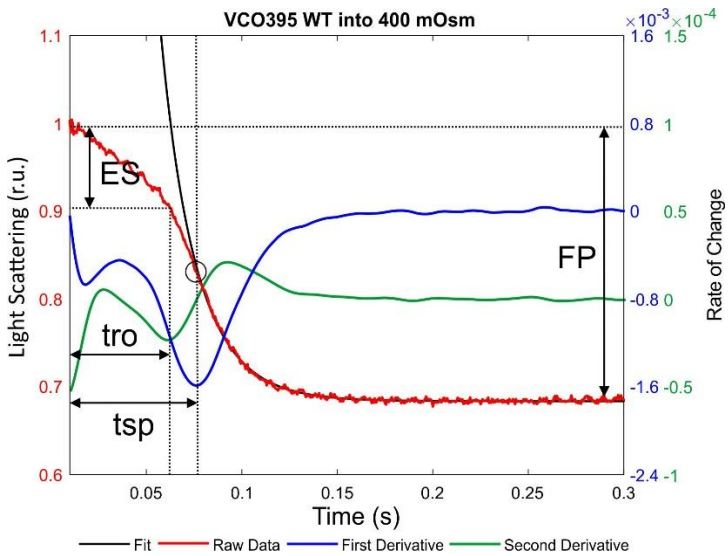


Figure 2. Representative scattering trace recorded in WT *V. cholerae* O395 that has been separated into distinct segments using derivative minima and fitting. The parameters such as time to release onset (tro, the minimum of the second derivative), extent of swelling (ES), time to the steepest point (tsp), fraction of permeable osmolytes (FP), and slope at the end are easily quantifiable via the first (blue) and second (green) derivatives. The rate of release is extracted from fitting the release phase with the simplified Rayleigh-Gans equation (black line).

Figure 3 compares side-by side traces recorded in single KO strains versus the WT O395 strain. With all cultures, the "no shock" control traces where the cells are rapidly mixed with the 1200 mOsm 'supernatant' growth medium were flat. A qualitative observation between representative

Δ*mscL* and WT scattering traces shows no sizable differences in the rates of osmolyte release throughout all magnitudes of down-shock (Figure 3A). Note that in the Δ*mscL* mutant, MscS is the dominant channel. We also observe similar trends in the end level reflecting the fraction of permeable osmolytes for the majority of down-shocks between WT and the Δ*mscL* mutant. For most shocks, by the 150 ms time point the scattering level is stabilized indicating that the release phase is over and tension has dropped to the threshold level for all MS channels in the population. However, two interesting differences can be seen at shocks to 900 mOsm and 400 mOsm. At down-shocks to 900 mOsm, WT appears to release less osmolytes overall than the Δ*mscL* clone, while the reverse is true at 400 mOsm (Figure 3A).

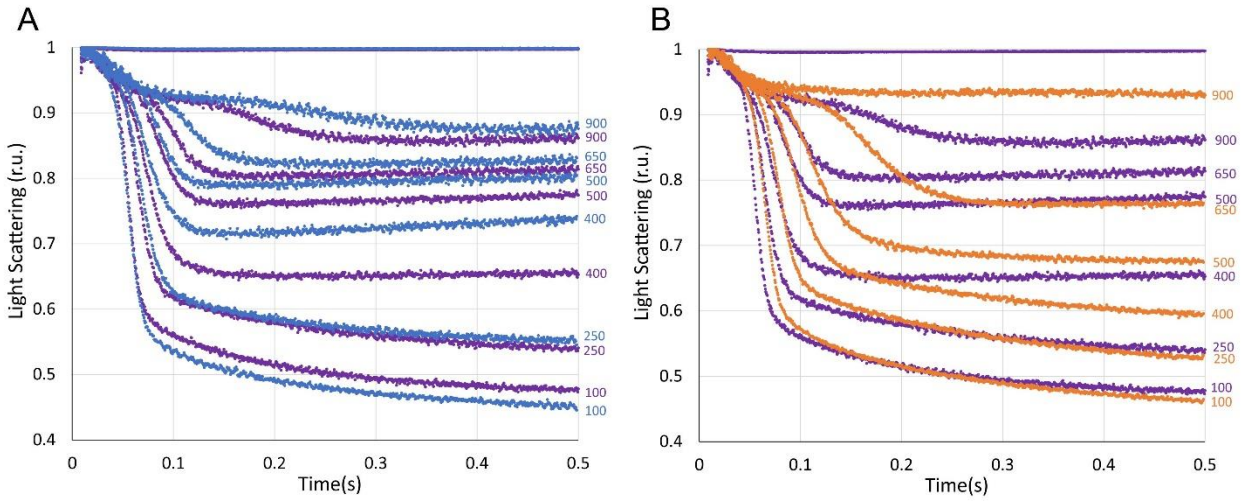


Figure 3. Light-scattering stopped-flow recorded in the range of osmotic downshifts from 1200 to 100 mOsm. The traces recorded in WT *V. cholerae* are shown in purple. (A) WT cells versus Δ*mscL* mutant (blue). (B) WT versus Δ*mscS* mutant (orange). Note that the presence of high-threshold MscL as a dominant channel in the Δ*mscS* strain results in a slightly delayed onset of release and a stronger incline at the right end of the trace signifying incomplete resealing.

Converse to that of the Δ*mscL* mutant, we observed that under osmotic down-shock, Δ*mscS* showed a delayed onset of downward deflection reflecting delayed channel openings with apparently higher tension threshold (MscL is the dominant valve) and slightly slower osmolyte release rates compared to WT *V. cholerae* O395. At intermediate magnitudes of shocks, the Δ*mscS* clone also appeared to expel a higher percentage of osmolytes than WT, as judged by the difference in scattering at comparable levels of shock. The faster and slightly deeper release in WT well correlates with its much higher survival rate especially at intermediate shocks relative to Δ*mscS* (see Figure 5 below).

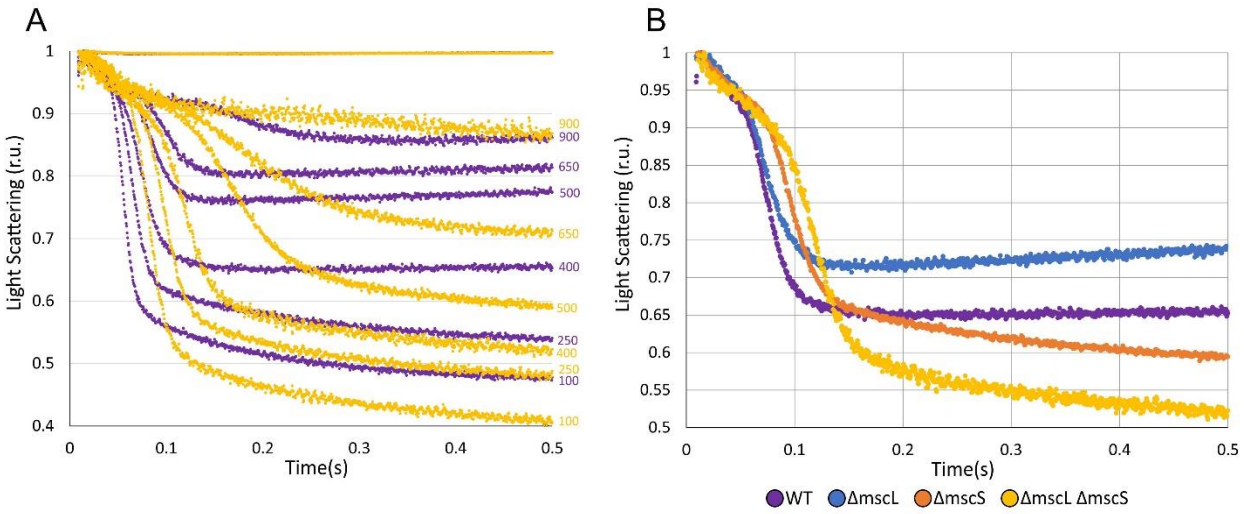


Figure 4. Light-scattering stopped-flow experiments comparing different strains. (A) Comparison of traces for the WT strain (purple) versus the double KO Δ*mscS*Δ*mscL* strain (yellow). All traces were recorded under identical conditions in the range of osmotic downshifts from 1200 to 100 mOsm as indicated by the traces. (B) Comparison of traces recorded under the same 1200 to 400 mOsm in WT *V. cholerae* cells (purple), Δ*mscL* (blue), Δ*mscS* (orange) and the double KO Δ*mscS* Δ*mscL* strain (yellow). Note negative incline of traces signifying continuing leakage from Δ*mscS* and double KO cells.

Upon deletion of both major release valves, the Δ*mscL* Δ*mscS* mutant exhibits a qualitative change in the scattering traces (Figure 4A). We should keep in mind that in this strain several minor MscS-like channels can still be expressed (Figure 1E) and may contribute to the release rate, but cannot impart high osmotic viability as we will see from Figure 5. We found that the double KO strain exhibits a dramatically slower and more gradual release process. The traces do not show a typical sharp 'break point' as there is no sufficient population of channels that would synchronously activate at a given tension. The smooth break of the curve at high shock magnitudes instead reflects the formation of non-specific 'cracks' in the membrane. WT traces clearly indicate that at intermediate shocks the release process is complete by 150-200 ms. The analysis of entire 4 s traces of the double KO strain shows that at intermediate shocks osmolyte release does not stabilize until closer to 1.5 seconds following mixing. At high magnitudes of down-shock, to 500 mOsm and lower, the osmolyte release never appears to stabilize (Figure 4A). This strongly suggests that the release in Δ*mscL*Δ*mscS* takes place through non-specific membrane 'cracks' which do not close or reseal. This pattern correlates with a drastic loss of viability (Figure 6).

Figure 4B directly compares traces recorded recorded under identical 1200 to 400 mOsm downshifts in all four strains. We see that WT O395 cells are the most fit in terms of their pre-release swelling is small, the release phase is fast (~30 ms), they efficiently expel 11% of internal osmolytes, and they perfectly reseal. The Δ*mscL* strain carrying active MscS responds similarly fast and stabilizes well after the shock even exhibiting a small upward drift likely reflecting slow cell shrinkage after osmolyte and water release. The absence of the large channel, however, apparently changes the repertoire of permeable osmolytes and thus the fraction released at the end is smaller. The Δ*mscS* strain carrying active MscL shows a delayed activation, larger pre-release swelling and a prominent downward creep at the end of the trace indicating continuing release.

The most 'fragile' double KO Δ*mscS* Δ*mscL* strain shows the highest extent of pre-release swelling which appears to be the major membrane-damaging factor. Correspondingly, the release through non-specific membrane cracks is slower and never stops within the time scale of seconds.

All stopped-flow traces were fitted using MATLAB (Figure 2) to extract the rate of release, time to steepest point and the fraction of released osmolytes. The averages and standard deviations are plotted against the magnitude of osmotic shock and compared across all *V. cholerae* O395 WT and MS channel KO strains in Figure 5. We found that there was no statistical difference between the release rates of Δ*mscL* mutant and WT *V. cholerae* at most down-shocks, with one exception. As noted in Figure 6E, we see the largest difference between all mutants at intermediate magnitudes of down-shock, such as shocks to 400 mOsm. As expected, the double MS channel KO, Δ*mscL* Δ*mscS*, had the slowest rates and a very gradual release consistent with a very different nature of permeation sites, which are likely tension-generated non-specific cracks rather than mechanosensitive channels.

We also examined the derivative of scattering changes for the maximum steepest negative point and time at which this occurred (Figure 2). This parameter suggested that at intermediate shocks (400 mOsm), the Δ*mscL* mutant likely has less active channels on average than other mutants. Yet, both WT and the Δ*mscL* mutant have comparably short times to the point of steepest slope at a majority of down-shocks (Figure 5C). The Δ*mscS* and double KO Δ*mscL* Δ*mscS* mutants, however, are both significantly slower than WT and Δ*mscL* to maximum channel activation.

The fractions of osmolytes that permeated through opened MS channels upon down-shock were also determined through the same fitting equation to stopped-flow data as release rates. At moderate shocks to 650 – 400 mOsm, Δ*mscS* and Δ*mscL* Δ*mscS* consistently released a higher fraction of permeable osmolytes than both Δ*mscL* and WT. This shows that MscS provides the most 'economical' regime of turgor adjustment. The two MscS-lacking mutants exhibited relatively similar percentages of permeable osmolytes at comparable shock levels to each other overall, though as we saw from shocks to 400 mOsm, the double Δ*mscL* Δ*mscS* KO clone continues to lose osmolytes until the end of the traces while the Δ*mscS* clone does not (see Figure 5F). At large shocks from to 1200 mOsm down to 250 or 100 mOsm, which was always associated with higher death rate across the strains, *V. cholerae* O395 WT and MS channel KO clones exhibited a similar trend (Figure 5D) showing a relatively steady increase in permeable osmolyte fraction. Again, this is likely due to the large contribution of leaking osmolytes from 'cracks' in damaged membranes, as this is a lethal shock.

To correlate the kinetic parameters of release with osmotic survival, all strains were subjected to osmotic viability assays. Surprisingly, these assays demonstrated a higher survival percentage under osmotic down-shock in Δ*mscL* than observed in WT *V. cholerae* (Figure 6). This increased survival occurred most prominently with large magnitudes of down-shocks (800 – 950 mOsm). The Δ*mscL* strain exhibited a remarkable survival rate which went below 50% only when cells were down-shocked to an osmolarity of 200 mOsm or below. The Δ*mscS* strain carrying active MscL, in contrast, suffered almost complete death at shocks to 400 mOsm. This result illustrates that MscL alone is not only insufficient to rescue the cells in this regime, but that alone it becomes toxic under moderate shocks in the absence of MscS. This is highly consistent with the recent results published for *E. coli* (Moller et al., 2023) and supports the idea that MscS with its distinctive ability to inactivate helps terminate the massive permeability response by driving tension away from the MscL threshold. At stronger shocks, however, MscL provides some advantage as a small number of Δ*mscS* colonies are always found persisting in the shock plates.

As predicted based on stopped-flow data, both Δ*mscS* and the double KO Δ*mscL* Δ*mscS* strains were observed to have a much lower tolerance for osmotic down-shock than WT (Figure 6).

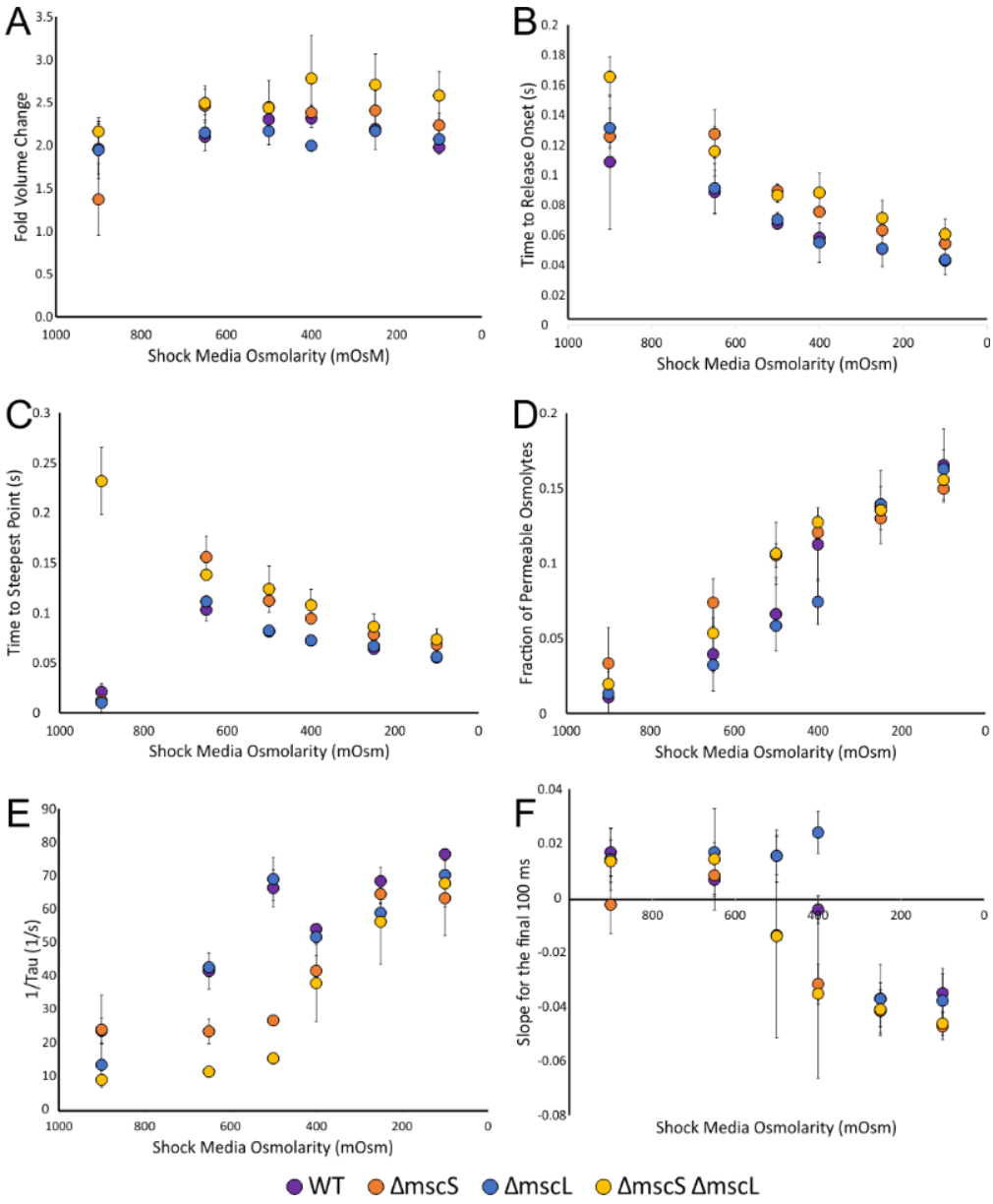


Figure 5. Kinetic parameters extracted from the stopped-flow traces *V. cholerae* O395 and the MS channel deletion mutants. Stopped-flow traces were fit to a modified Rayleigh-Gans equation from initialization of MS channel openings to the point of channel closure as described in Figure 2. These fits were averaged (n=4-5) and used to determine the osmolyte release rate under down-shocks from 1200 mOsm LB to the media osmolarity indicated on the x-axis. Error bars represent standard deviation. (A) The volume fold change as the cell swells in response to hypoosmotic shock. (B) Time to release onset corresponds to the time spent swelling until sufficient turgor pressure is achieved to activate channels. (C) Time to steepest point is the time at which the fastest scatter change occurred for each level of down-shock, indicating the time until maximum channel activity. (D) Fraction of permeable osmolytes released from *V. cholerae*

O395. (E) The rate of osmolyte release. (F) The slope for the final 100 ms is a measure of membrane resealing. A positive slope is an indicator of good resealing, whereas a negative slope indicates the imperfect resealing that results in leaks through non-inactivating channels or nonspecific cracks.

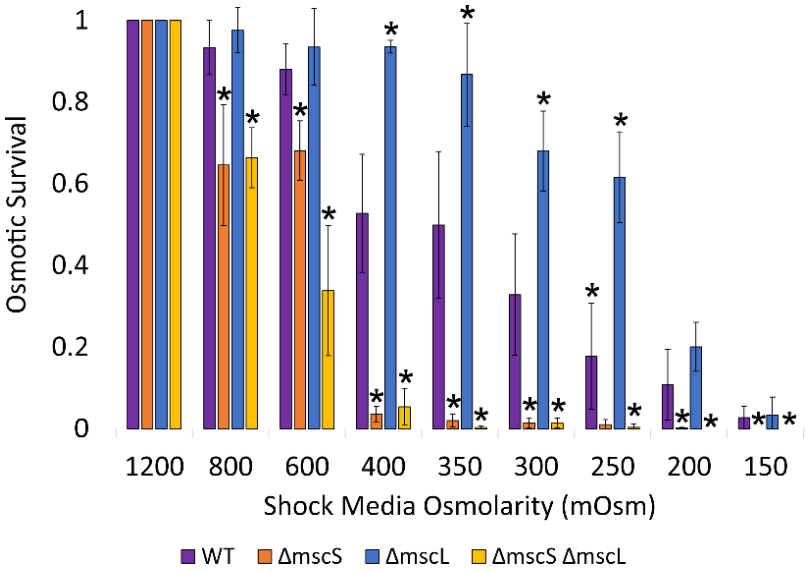


Figure 6. Osmotic viability of WT and KO mutants. Osmotic survival of channel KOs. All samples were plated after osmotic shock from 1200 mOsm to the value indicated on the x-axis and survival measured by CFU's/mL. Error bars represent standard deviation of each averaged sample (n=5-15). The mscS gene was transformed into the pBAD vector and complimented into ΔmscS demonstrating some improved survivability (statistically significant at 400, 350, and 300 mOsm). All averages and standard deviations of kinetic parameters were results of 6-7 independent stopped-flow trials (n=6-7).

The predictions of kinetic modeling.

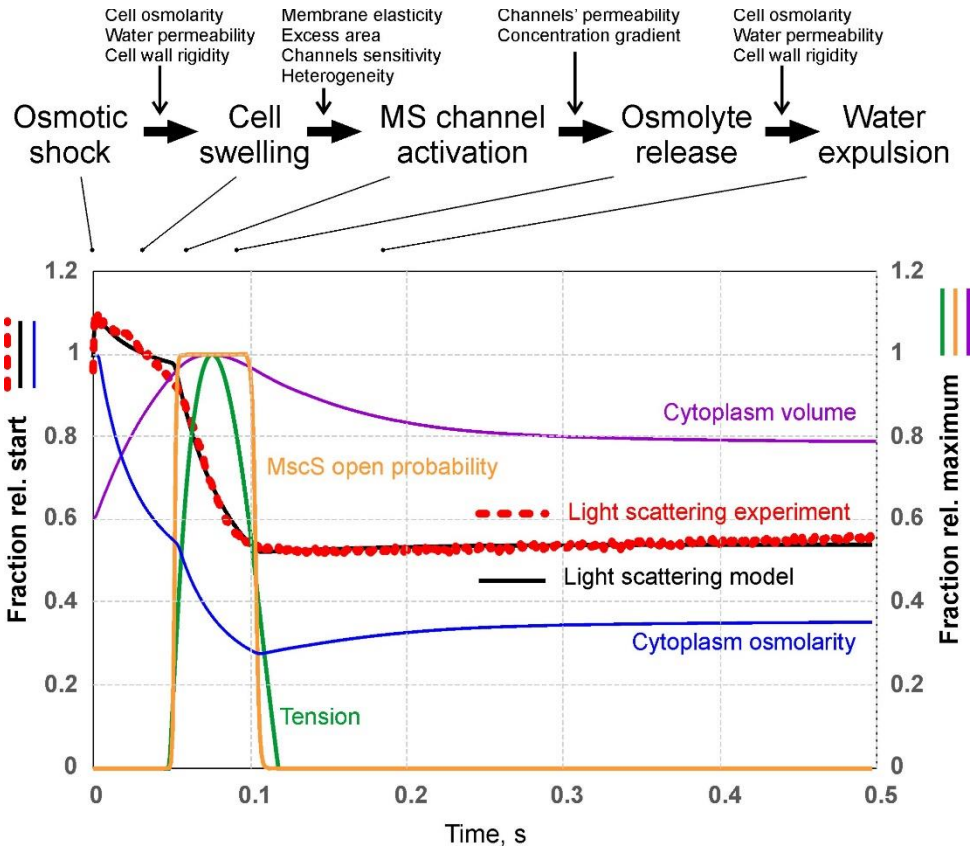


Figure 7. Kinetic model of *V. cholerae* response to osmotic down-shock (300 mOsm) in the absence of MscL. The model was developed using COPASI software. The parameters of the model were based on our measurements of cell volume distribution, water permeability, and MscS gating parameters, supplemented with data from literature, and adjusted to optimize the fit to the measured changes in optical properties of the suspension. Light-scattering estimates were performed in Rayleigh-Gans approximation.

## Discussion

Vibrio cholerae, a typical estuarial marine bacterium, becomes a deadly pathogen when it acquires and incorporates a complex of virulence genes horizontally passed through phages or plasmids. The high adaptability of this organism to a variety of environments from concentrated high-osmotic gut content to rainwater facilitates its environmental stability and transmission producing outbreaks. This osmotic stability is imparted by a set of tension-activated mechanosensitive channels that function as osmolyte release valves and quickly dissipate excessive osmotic gradients to rescue cells from lysis. The two major contributors to osmotic permeability are the low-threshold channel MscS and high-threshold MscL. When the knock-out strains were first generated and functionally characterized, there was the impression that MscS and MscL are partially redundant and rescue shocked cells equally well (Levina et al., 1999). Subsequent studies have shown that the two channels are not redundant and work in tandem (Moller et al., 2023).

In contrast to MscL, which behaves as a two-state channel, MscS has the ability to inactivate from the closed state under moderate near-threshold tensions. In *E. coli*, this distinctive property of MscS fulfills the special function of terminating the massive permeability response when tension drops down to MscS's activation threshold. The mere presence of MscS at the end of the permeability response also silences the flickery MscL channel by driving tension below its activation threshold. In the absence of MscS, MscL stabilizes tension near its own threshold of ~10 mN/m and remains in its low-open-probability state preventing membrane resealing. This is precisely the picture that we now observe in *V. cholerae*.

The engineered Δ*mscS*, Δ*mscL*, and the double Δ*mscS* Δ*mscL* KO strains from WT *V. cholerae* O395 revealed clear and correlated electrophysiological, release kinetic and survival phenotypes. The severely compromised survival of the double KO strain can be directly linked to the minute population of remaining tension-activated channels (Figure 1F) incapable of producing a robust permeability response that would prevent the excessive swelling observed in scattering traces. This swelling produces a non-resealing and perpetually leaking membrane. The poorly surviving Δ*mscS* strain shows a nearly normal degree of swelling which should not lead to mechanical rupture of the cell, but instead the traces reveal an inclined end-level indicating a leaky (non-sealed) state of the membrane due to the inability of dominant MscL to close completely or inactivate. The high survival of the Δ*mscL* strain, comparable and even exceeding that of WT, shows that early activation of release valves is highly beneficial for curbing the pressure surge. Furthermore, its ability to inactivate (Rowe et al., 2013) provides a firm termination mechanism. The mechanosensitive channel of small conductance (MscS) has an unexpectedly strong impact on survival and is overexpressed in the Δ*mscL* strain suggesting a functional and transcriptional cross-talk between the two major osmolyte release valves. A similar effect of *mscL* deletion on the level of *mscS* mRNA was recently observed in *E. coli* (Moller et al., 2023).

We argue that the MscS channel that is capable of inactivation is a critical component of the release system allowing for proper termination of the hypoosmotic response. Moreover, if a Δ*mscL* mutant survives abrupt down-shocks even better than a strain with both channels, then why is MscL needed and preserved in evolution? We presume that the presence of a high-threshold non-inactivating channel such as MscL is therefore equally important. While the Δ*mscL* mutant demonstrates increased survival under single down-shock events, substantial inactivation of the MscS population under a graded shock scenario is possible. For instance, a prolonged exposure to a moderately hypoosmotic medium (pre-shock) would lead to massive inactivation of MscS, leaving *V. cholerae* susceptible to membrane damage under further stronger down-shocks. The presence of the non-inactivating MscL population eliminates this risk.

How quickly does the release mechanism respond to a sudden medium dilution? Our data shows that under extreme shocks, cells swell within 40 ms and release up to 17% of their dry weight within the next 20 ms. The best osmotic survival correlated with low ES, short tro and tsp and, importantly, lowest slope at the end.

The stopped-flow data now allow for kinetic modeling of the *Vibrio* osmotic permeability response and its rescuing. The simplified MscS-only expressing strain (*ΔmscL*) allows for a reconstruction of the events that take place *in vivo*, which include (1) initial swelling producing distension of the peptidoglycan and outer membrane and complete unfolding of the inner membrane, (2) generation of tension in the inner membrane which activates MS channels as soon as it reaches the threshold, (3) a fast osmolyte release phase, (4) the following process of water expulsion, and (5) slower volume/concentration adjustments possibly related to the recoil of the stretched peptidoglycan. The kinetic model of the swelling-release cycle presented in Figure 9

includes realistic parameters of *Vibrio* cell area and volume, elastic properties of the peptidoglycan, the excess of the inner membrane area, permeability of cell envelope for water, tension activation slopes and midpoints for channels and their combined permeability. The model programmed in the kinetic modeling suite *COPASI* (Mendes et al., 2009) explicitly takes into account refractive index of cells and, as seen from the figure, it well reproduces the experimental time course of scattering.

We conclude that the osmotic rescuing in *Vibrio cholerae* is a kinetics-based mechanism where the two mechanosensitive channels, MscS and MscL, act in tandem. While the functional interaction between these two structurally unrelated species still needs to be explored in more detail, our data shows that MscS is the most important component of the system and that it can fulfill its rescuing function by itself. MscL is never found in any species alone because it requires MscS for proper termination of the osmotic permeability response.

Acknowledgements

This research was supported by NIH R01AI135015 to SS. This research was also supported in part by a grant to the University of Maryland from the Howard Hughes Medical Institute through the Science Education Program.
We thank Anthony Schams for assistance with stopped-flow MATLAB fitting and analysis. We also thank Dr. Ugur Çetiner for his correspondence assisting in interpreting up-shock stopped-flow data and advice on calculating water permeability coefficients.

References


Akitake, B., A. Anishkin, and S. Sukharev. 2005. The "dashpot" mechanism of stretch-dependent gating in MscS. *J.Gen.Physiol*. 125:143-154.

Balleza, D., and F. Gomez-Lagunas. 2009. Conserved motifs in mechanosensitive channels MscL and MscS. *Eur.Biophys J*.

Belyy, V., K. Kamaraju, B. Akitake, A. Anishkin, and S. Sukharev. 2010. Adaptive behavior of bacterial mechanosensitive channels is coupled to membrane mechanics. *J Gen Physiol*. 135:641-652.

Bialecka-Fornal, M., H.J. Lee, and R. Phillips. 2015. The rate of osmotic downshock determines the survival probability of bacterial mechanosensitive channel mutants. *Journal of bacteriology*. 197:231-237.

Booth, I.R., and P. Blount. 2012. The MscS and MscL families of mechanosensitive channels act as microbial emergency release valves. *Journal of bacteriology*. 194:4802-4809.

Cetiner, U., I. Rowe, A. Schams, C. Mayhew, D. Rubin, A. Anishkin, and S. Sukharev. 2017. Tension-activated channels in the mechanism of osmotic fitness in Pseudomonas aeruginosa. *J Gen Physiol*. 149:595-609.

Cox, C.D., N. Bavi, and B. Martinac. 2018. Bacterial Mechanosensors. *Annu Rev Physiol*. 80:71-93.

Emch, M., C. Feldacker, M.S. Islam, and M. Ali. 2008. Seasonality of cholera from 1974 to 2005: a review of global patterns. *Int J Health Geogr*. 7:31.

Faruque, S.M., M.J. Albert, and J.J. Mekalanos. 1998. Epidemiology, genetics, and ecology of toxigenic Vibrio cholerae. *Microbiol Mol Biol Rev*. 62:1301-1314.

Hase, C.C. 2001. Analysis of the role of flagellar activity in virulence gene expression in Vibrio cholerae. *Microbiology (Reading)*. 147:831-837.

Hoops, S., S. Sahle, R. Gauges, C. Lee, J. Pahle, N. Simus, M. Singhal, L. Xu, P. Mendes, and U. Kummer. 2006. COPASI--a COmplex PAthway SImulator. *Bioinformatics*. 22:3067-3074.

Keymer, D.P., M.C. Miller, G.K. Schoolnik, and A.B. Boehm. 2007. Genomic and phenotypic diversity of coastal Vibrio cholerae strains is linked to environmental factors. *Appl.Environ.Microbiol.* 73:3705-3714.

Koch, A.L. 1961. Some Calculations on Turbidity of Mitochondria and Bacteria. *Biochimica Et Biophysica Acta*. 51:429-&.

Koch, A.L., B.R. Robertson, and D.K. Button. 1996. Deduction of the cell volume and mass from forward scatter intensity of bacteria analyzed by flow cytometry. *J Microbiol Meth*. 27:49-61.

Kung, C., B. Martinac, and S. Sukharev. 2010. Mechanosensitive channels in microbes. *Annu.Rev.Microbiol.* 64:313-329.

Levina, N., S. Totemeyer, N.R. Stokes, P. Louis, M.A. Jones, and I.R. Booth. 1999. Protection of Escherichia coli cells against extreme turgor by activation of MscS and MscL mechanosensitive channels: identification of genes required for MscS activity. *EMBO J.* 18:1730-1737.

Martinac, B., M. Buechner, A.H. Delcour, J. Adler, and C. Kung. 1987. Pressure-sensitive ion channel in Escherichia coli. *Proc.Natl.Acad.Sci.U.S.A.* 84:2297-2301.

Mendes, P., S. Hoops, S. Sahle, R. Gauges, J. Dada, and U. Kummer. 2009. Computational modeling of biochemical networks using COPASI. *Methods Mol Biol*. 500:17-59.

Moller, E., M. Britt, A. Schams, H. Cetuk, A. Anishkin, and S. Sukharev. 2023. Mechanosensitive channel MscS is critical for termination of the bacterial hypoosmotic permeability response. *J Gen Physiol*. 155.

Nahar, S., M. Sultana, M.N. Naser, G.B. Nair, H. Watanabe, M. Ohnishi, S. Yamamoto, H. Endtz, A. Cravioto, R.B. Sack, N.A. Hasan, A. Sadique, A. Huq, R.R. Colwell, and M. Alam. 2011. Role of Shrimp Chitin in the Ecology of Toxigenic Vibrio cholerae and Cholera Transmission. *Front Microbiol*. 2:260.

Pflughoeft, K.J., K. Kierek, and P.I. Watnick. 2003. Role of ectoine in Vibrio cholerae osmoadaptation. *Appl.Environ.Microbiol.* 69:5919-5927.

Rowe, I., M. Elahi, A. Huq, and S. Sukharev. 2013. The mechanoelectrical response of the cytoplasmic membrane of Vibrio cholerae. *J Gen Physiol*. 142:75-85.

Sukharev, S. 2002. Purification of the small mechanosensitive channel of Escherichia coli (MscS): the subunit structure, conduction, and gating characteristics in liposomes. *Biophys.J.* 83:290-298.

Sukharev, S.I., P. Blount, B. Martinac, F.R. Blattner, and C. Kung. 1994. A large-conductance mechanosensitive channel in E. coli encoded by mscL alone. *Nature*. 368:265-268.

Sukharev, S.I., B. Martinac, V.Y. Arshavsky, and C. Kung. 1993. Two types of mechanosensitive channels in the Escherichia coli cell envelope: solubilization and functional reconstitution. *Biophys J*. 65:177-183.

Sukharev, S.I., W.J. Sigurdson, C. Kung, and F. Sachs. 1999. Energetic and spatial parameters for gating of the bacterial large conductance mechanosensitive channel, MscL. *J.Gen.Physiol*. 113:525-540.

Ushijima, B., P. Videau, D. Poscablo, J.W. Stengel, S. Beurmann, A.H. Burger, G.S. Aeby, and S.M. Callahan. 2016. Mutation of the toxR or mshA genes from Vibrio coralliilyticus strain OCN014 reduces infection of the coral Acropora cytherea. *Environ Microbiol*. 18:4055-4067.

Wood, J.M. 2006. Osmosensing by bacteria. *Sci.STKE.* 2006:e43.

Yancey, P.H., M.E. Clark, S.C. Hand, R.D. Bowlus, and G.N. Somero. 1982. Living with water stress: evolution of osmolyte systems. *Science*. 217:1214-1222.